IEICE TRANS. FUNDAMENTALS, VOL.E88–A, NO.3 MARCH 2005

PAPER

# Acquisition and Modeling of Driving Skills by Using Three Dimensional Driving Simulator

**Jong-Hae KIM**[†a)], **Yoshimichi MATSUI**[†], *Nonmembers*, **Soichiro HAYAKAWA**[††], **Tatsuya SUZUKI**[†††], *Members*, **Shigeru OKUMA**[†], *Nonmember*, *and* **Nuio TSUCHIDA**[††], *Member*

**SUMMARY** This paper presents the analysis of the stopping maneuver of the human driver by using a new three-dimensional driving simulator that uses CAVE, which provides stereoscopic immersive vision. First of all, the difference in the driving behavior between 3D and 2D virtual environments is investigated. Secondly, a GMDH is applied to the measured data in order to build a mathematical model of driving behavior. From the obtained model, it is found that the acceleration information has less importance in stopping maneuver under the 2D and 3D environments.

***key words:*** *CAVE, virtual reality, stereoscopic immersive vision, GMDH, driving skill*

## 1. Introduction

Recently, traffic systems centered on vehicles have been changing rapidly as computer and communications technologies have advanced. Thus far, vehicle controls have been used to improve vehicle performance. However, due to the variety of customer demands, it has become problematic to design and manufacture vehicles to meet every customer's preferences. To satisfy the various requirements of all customers, it is necessary to understand the driving skills of each type of driver, and then to incorporate that understanding into the design of vehicle control system [1]. This is an important undertaking, especially for vehicles that will be driven by the elderly or the disabled. To reflect on driving skills, it is first necessary to measure them. In a real environment, two significant problems occur in measuring driving skills: (1) Many sensors must be used in order to detect information from or about the driver and the environment, and (2) The driver may have to face dangerous situations, such as a collision with another vehicle, to acquire skills for collision avoidance. One promising way to overcome these difficulties is to use a driving simulator (DS) [2]–[6]. However, most conventional simulators provide the driver with only two-dimensional (2D) visual images. This renders the measured data on driving skills less reliable. Moreover, no quantitative comparison of the driving behavior under the 2D and 3D virtual environments has been found in the past literature.

In this paper, first of all, a three-dimensional (3D) DS using CAVE, which provides stereoscopic immersive vision, is developed. Based on the developed DS, difference in the driving behavior between 3D and 2D virtual environments are quantitatively measured with focusing on the drivers' ability to stop in front of a stop line. Secondly, an analytical model of the stopping maneuver is built. In modeling driving behavior, the following two significant problems are studied.

1) How to find a mathematical structure of the driving behavior.

2) How to select the necessary information as inputs to the driver.

In order to solve these problems, a Group Method of Data Handling (GMDH) is introduced and is applied to the measured data. The results show the dependence of driving behavior on physical variables. Although the rigorous understanding of each term in the GMDH model is somewhat unclear, the GMDH can be used to capture the meaning of driving behavior at least roughly associating with each variable.

This paper is organized as follows. In Sect. 2, configuration of the developed DS based on CAVE is introduced. In Sect. 3, the scenario of our examination is described. In Sect. 4, based on the setup described in Sect. 3, differences in driving behavior between 3D and 2D virtual environments are shown and analyzed. In Sect. 5, the GMDH is applied to the measured data in order to build a mathematical model of the driver's behavior.

## 2. Configuratoin of Driving Simulator

### 2.1 CAVE

CAVE is a virtual reality device developed by researchers at EVL (Electronic Visualization Laboratory) of the University of Illinois at Chicago. CAVE provides the 3D virtual environment. Our CAVE is able to project the 3D CG image on four screens around the user (one in the front, one on the floor, and two on the sides) in a 3m cubic space. The projection in the CAVE system is controlled by SGI ONYX2 image generator. The maximum ONYX2 image frame rate used in the experiment is 25 [frame/sec]. One of the sig-

Manuscript received November 13, 2003.
Manuscript revised July 29, 2004.
Final manuscript received November 19, 2004.

[†]The authors are with the Department of Electrical Engineering and Computer Science, Graduate School of Engineering, Nagoya University, Nagoya-shi, 468-8603 Japan.
[††]The authors are with Toyota Technological Institute, Nagoya-shi, 468-8511 Japan.
[†††]The author is with the Department of Electronic-Mechanical Engineering, Graduate School of Engineering, Nagoya University, Nagoya-shi, 468-8603 Japan.
a) E-mail: kimjh@okuma.nuee.nagoya-u.ac.jp

DOI: 10.1093/ietfec/e88–a.3.770

nificant characteristics of CAVE is that the projected image varies according to the viewpoint and motions of the driving examinee, by using a magnetic position sensor mounted on 3D visual goggles. This enables the examinee to see quite natural 3D visual images in real time without feeling any incongruence. Moreover, CAVE can easily switch the projected image between 3D and 2D. This enables us to investigate the difference between 2D and 3D projection. Also, Performer software is adopted as a graphics library for the CAVE system. Performer is not only suitable for real-time processing, but also easy to link to other commercial 3D object design software. By employing CAVE and Performer, the developed DS can provide driving environments that seem more natural than other conventional 2D vision-based DS.

### 2.2 Configuration of DS

The configuration and appearance of the driving simulator based on CAVE are shown in Figs. 1(a) and (b). The display unit in the CAVE system provides the 3D virtual environment, and it is controlled by the ONYX2. The display program was developed by making use of the CAVE library and Performer. The cockpit is built by installing a real steering wheel, an accelerator and a brake in the CAVE system. The informations on the input from the driver to the steering wheel, accelerator and brake are transferred to the PC through USB terminal, and the vehicle position and motion

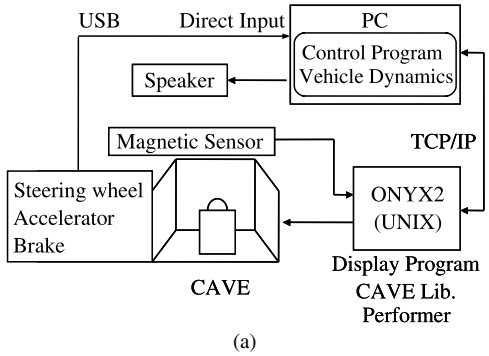


(a)

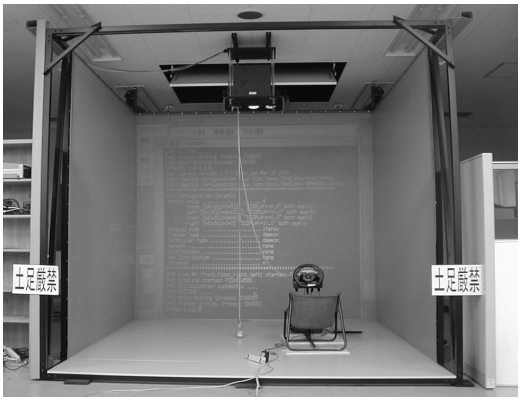


(b)

**Fig. 1** The developed driving simulator. (a) Configuration of the DS. (b) CAVE system.

are calculated based on these inputs and vehicle dynamics implemented on the PC.

The results of the calculation are transferred to ONYX2 through the Internet (TCP/IP), and the 3D visual image based on the position and motion of the vehicle is displayed.

## 3. Capturing Driving Behavior

### 3.1 Road Environments and Behavior

Generally speaking, most traffic accidents occur at intersection. The driving behavior at intersection can be divided into three typical behaviors [7], [8]:

(i) Going straight and crossing the intersection
(ii) Starting and stopping in front of a stop line
(iii) Turning right or left at the intersection

In this paper, we focus on stopping maneuver [9]–[14], (ii) because the difference between 3D and 2D virtual environments is more emphasized in this behavior than in the others [15], [16]. In order to model the driving behavior, the following sensory information is captured as the inputs:

(i) Distance from the front end of the vehicle to the stop line [$x_1$]
(ii) First time derivative of (i) (velocity) [$x_2$]
(iii) Second time derivative of (i) (acceleration)[$x_3$]

The outputs of the driver are also specified as follows:

(i) Accelerator output [$y_1$]
(ii) Brake output [$y_2$]

Generally, it is desirable to use accelerator pedal stroke [%] and brake pedal force [$N$] to express the measurements of "accelerator output [$y_1$]" and "brake output [$y_2$]." Actually, these variables ($y_1$, $y_2$) indicate accelerator pedal stroke [%] and brake pedal pressure [MPa] ([N/mm$^2$]) in this paper. Also, braking amount depicted in Figs. 5 and 6 is magnified by 100.

Note that no steering operation is necessary in the stopping maneuver.

The configuration of the model of the intersection and its projected image are shown in Figs. 2(a) and (b) with some geometric parameters.

The road is 7 m wide and the pedestrian way is 2 m wide. There are two intersections in this environment (A and B). The driver is supposed to stop in front of the stop line at the intersection (A). The vehicle is supposed to start moving at position (a or b). Profiles of driving data are obtained for both 3D and 2D virtual environments.

### 3.2 Driving Conditions

The vehicle used in the simulator is a sedan type whose engine displacement is 1800 cc. The bonnet of the vehicle can be seen from the driver. Four male drivers who have driver's licenses, ranging in age from 22 to 40 years, are selected as examinees. All examinees did not know the purpose of this experiment and we did not allow them to have any knowledge regarding this study. They also had never driven on the simulator before. The maximum velocity is set at 40 km/h

or 60 km/h, and the selected starting point is 0 m or 50 m as shown in Fig. 2(a).

Each driver takes a number of preliminary trials to get used to the DS, then begins the test, which is made up of numerous trials. The number of trials for each driver is listed in Table 1.

### 3.3 Experimental Procedures

To begin with, both preliminary trials and actual test trials under the 2D virtual environment are carried out 40 times and 20 times, respectively. These trials consist of four different driving situations (with 10 practice and 5 actual trials per situation):

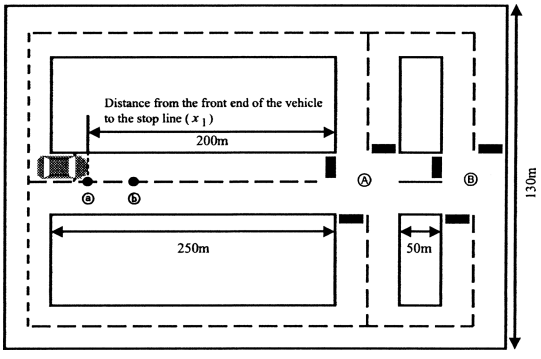


(a)

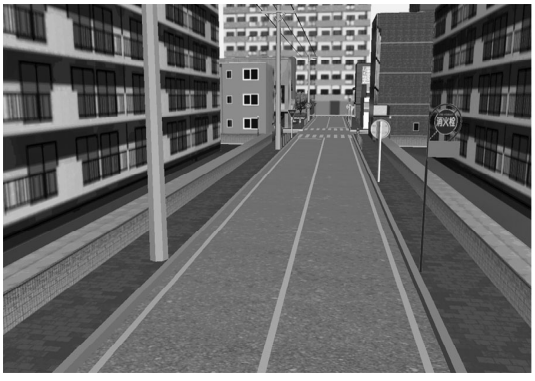

(b)

**Fig. 2** Approaching an intersection. (a) Model of intersection. (b) Sample of projected image.

**Table 1** Experimental conditions.

| Notation | Driving conditions(Maximum steady running velocity [km/h], start point [m] | | | |
|---|---|---|---|---|
| | 40 km/h 0 m | 40 km/h 50 m | 60 km/h 0 m | 60 km/h 50 m |
| Preliminary drive under 2D | Ten times | Ten times | Ten times | Ten times |
| Real drive under 2D | Five times | Five times | Five times | Five times |
| Preliminary drive under 3D | Ten times | Ten times | Ten times | Ten times |
| Real drive under 3D | Five times | Five times | Five times | Five times |

(1) Velocity restriction of 40 km/h, starting point of 0 m.
(2) Velocity restriction of 40 km/h, starting point of 50 m.
(3) Velocity restriction of 60 km/h, starting point of 0 m.
(4) Velocity restriction of 60 km/h, starting point of 50 m.

The experiments are executed above order. After the preliminary trials, the driver rests for 10 minutes, and answers a questionnaire in which the examinee record the usual driving behavior in real situation, driving preferences, SSSQ [17], [18], and so on. The SSSQ test is a way to find a driver who is likely to suffer from simulator sickness. If the driver wants to drop out of the experiment because of simulator sickness, the experiment is suspended. The experiment under the 3D virtual environment is carried out in the same way as the 2D virtual environment. Each driver takes about 80 minutes to complete all of the trials.

## 4. Comparison between 2D and 3D

Based on the setup described in Sect. 3, four drivers carried out the experiments under the 2D and 3D virtual environments. First of all, the differences in the stopping maneuver between the 3D and 2D virtual environments were investigated and analyzed. The personal information of four examinees are listed in Table 2.

The profiles of the driving data of the four drivers in the case of velocity restriction of 60 km/h are depicted in Fig. 3 (for the 2D and 3D environments, the first and third trials of each driver are depicted, respectively).

Figures (a) and (c) show the data for the 2D environment, while (b) and (d) show the data for the 3D. Also, Figs (a) and (b) correspond to the case of starting point of 0 [m]; (c) and (d) correspond to the case of starting point of 50 [m]. The horizontal and vertical axes denote the position (stop line is located at 200 m) and the velocity of the vehicle, respectively. Paying attention to the circle in each figure, we can determine that the driver can stop at the stopping point precisely under the 3D virtual environment (see Figs. (b) and (d)).

On the other hand, the driver feels difficulty in stopping precisely at the stop line under the 2D virtual environment. In order to analyze this result quantitatively, the measured final stopping points of each driver were collected, and their average and variance were calculated as listed in Table 3. The larger variance implies that the driver has more difficulty in precise stopping.

In Table 3, the variance in the 3D environment is smaller than in the 2D environment. This result comes from the fact that the human can sense the real 'distance' in the

**Table 2** Individual information of examinees.

| Examinee | Age [Years old] | Mileage per year [km] | Driving Career [Years] |
|---|---|---|---|
| E1 | 22 | 2500 | 4 |
| E2 | 40 | 20000 | 7 |
| E3 | 22 | 5000 | 3 |
| E4 | 22 | 20000 | 4 |

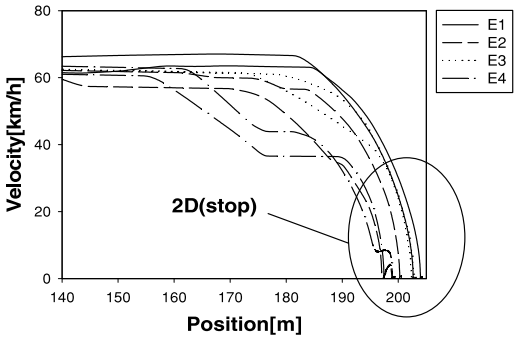


(a)

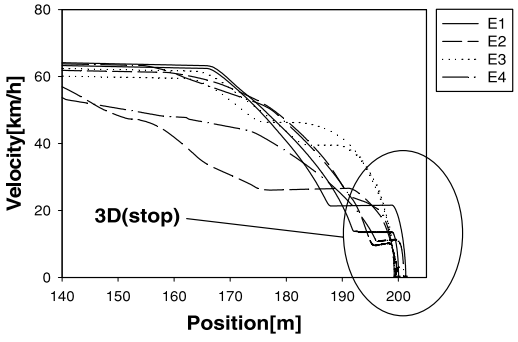


(b)

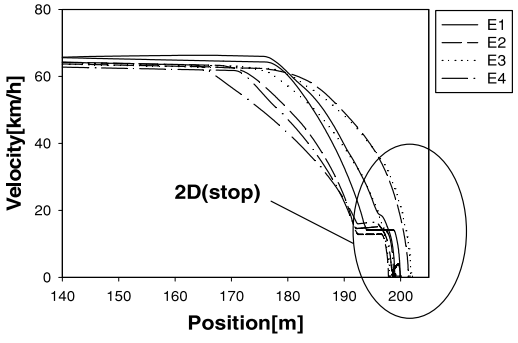


(c)

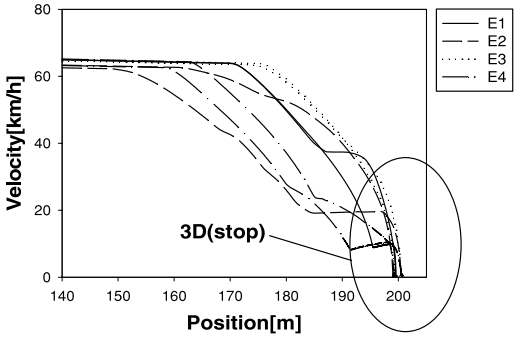


(d)

**Fig. 3** Behavior at stopping. (a) 2D (starting point of 0 [m]). (b) 3D (starting point of 0 [m]). (c) 2D (starting point of 50 [m]). (d) 3D (starting point of 50 [m]).

3D virtual environment, but not in the 2D.

Driver E4 shows very little difference in the variances between 3D and 2D, compared with other drivers (E1, E2, E3). Most likely, this is due to the simulator sickness mentioned in Sect. 3. Actually, driver E4 reported high levels of simulator sickness in our questionnaires. This result may also lead to an understanding of the ability of "space recognition" of the human driver. Also, in the case of 3D, the drivers are likely to stop several meters before the stop line, reaccelerate and finally stop at the line. As shown in Fig. 3, this kind of behavior is often observed in real situation. Moreover, in the 2D environment, deceleration begins later (at about 180 m) than it does in the 3D virtual environment (at about 170 m). In fact, it is well known that the deceleration in the real car begins earlier than it does in the conventional DS. From these considerations, we can conclude that the 3D virtual environment enables us to capture much more reliable information about the driver's skill than the 2D virtual environment.

**Table 3** Variance and average values of stopping point.

| Subject | Notation | | Driving conditions(Maximum steady running velocity [km/h], start point [m] | | | |
|---|---|---|---|---|---|---|
| | | | 40 km/h 0 m | 40 km/h 50 m | 60 km/h 0 m | 60 km/h 50 m |
| E1 | 2D | Av. | 200.19 | 199.81 | 201.87 | 200.58 |
| | | Va. | 0.149 | 0.169 | 5.752 | 0.823 |
| | 3D | Av. | 200.02 | 200.25 | 200.61 | 200.52 |
| | | Va. | 0.091 | 0.101 | 0.879 | 0.626 |
| E2 | 2D | Av. | 198.39 | 198.83 | 198.12 | 199.89 |
| | | Va. | 2.936 | 1.510 | 5.086 | 6.535 |
| | 3D | Av. | 201.23 | 200.31 | 200.16 | 200.14 |
| | | Va. | 2.141 | 0.380 | 0.220 | 0.504 |
| E3 | 2D | Av. | 199.15 | 200.57 | 200.89 | 198.96 |
| | | Va. | 1.359 | 3.021 | 3.770 | 1.669 |
| | 3D | Av. | 200.21 | 200.12 | 200.36 | 200.20 |
| | | Va. | 0.182 | 1.058 | 0.714 | 0.258 |
| E4 | 2D | Av. | 199.59 | 199.61 | 199.92 | 199.84 |
| | | Va. | 0.532 | 0.542 | 0.465 | 1.326 |
| | 3D | Av. | 200.17 | 200.36 | 200.26 | 200.24 |
| | | Va. | 0.528 | 0.496 | 0.447 | 0.482 |

## 5. Modeling by GMDH

In this section, we describe how to generate the mathematical model of driving behavior by using a Group Method of Date Handling (GMDH) under the definition of the input and output in Sect. 3.

A GMDH algorithms [19], [20] can be used both as a predictor for estimating the output of complex systems and for identification purpose in determining which input variables are important in the model. The advantage of the GMDH is emphasized especially when the system has high complexity, and the designer does not have any specific knowledge of the system in advance.

However, although the fitting of the model becomes well as the layer of the model evolves, it becomes difficult to understand the physical meaning of the model and the meaning of each term because the obtained model often results in too complicated model. This implies that the overfitting problem [22]–[24] must be addressed carefully in the GMDH. In the GMDH, this problem is recognized as the design problem of the regularity condition. In the following,

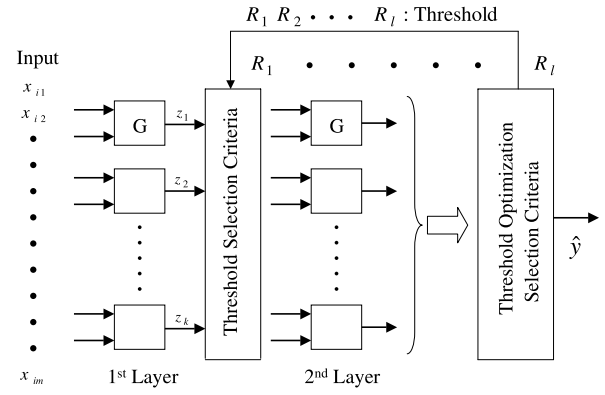


**Fig. 4** Block diagram of GMDH.

we describe the detail of the GMDH including the design of regularity condition.

Although there exists so many types of GMDH, the perceptron-type GMDH shown in Fig. 4 is used in this paper.

We assume that multi-input '$x_{i1}, x_{i2} \ldots, x_{im}$,' and single output '$y_{i+20}$' have the following relationship:

$$y_{i+20} = f(x_{i1}, x_{i2} \ldots, x_{im}) \tag{1}$$

The magnitude of the time lag 20 was specified by taking into account the time lap from the recognition to occurrence of some action in the human behavior. The existence of such time lag is widely known, and it varies from 100 [ms] to 300 [ms] in ordinal case [21]. Therefore, we have decided to adopt the above relationship by taking into account the sampling interval 10 [ms] (i.e. 200 [ms] time lap) in our experiment.

In Eq. (1), $f$ is an arbitrary polynomial expression, and m denotes the number of input variables. Also, $n$ denotes the number of measured data sets, and $l$ denotes the index of the layers in the GMDH.

The procedure to find the estimated model of (1) based on the perceptron-type GMDH is described as follows:

Let $x_{ij}$($i$=1,2,..., $n$, $j$=1,2,..., $m$) denote the $i$-th data of the $j$-th input variable, and $y_i$ denote the $i$-th data of the output.

**Step 1 :** Divide $n$ collected data into two sets, a "Training Data set" (TRD) and a "Checking Data set" (CHD). Note that TRD is used to estimate coefficients of partial descriptions defined in Step 2, and CHD is used to evaluate the accuracy of the estimated partial descriptions. Assume that the number of data in TRD and CHD are $n_{tr}$ and $n_{ch}$ ($n$= $n_{tr}$ + $n_{ch}$), respectively. Also, the TRD (about 70(%) of the total number of data) is a collection of data that have large variance, and the CHD (about 30(%) of the total number of data sets) is a collection of data that have small variance.

**Step 2 :** Consider the following partial descriptions, which consist of two inputs, $x_{ip}$ and $x_{iq}$ (G in Fig. 4):

$$z_k = A_{0k} + A_{1k}x_{ip} + A_{2k}x_{iq} + A_{3k}{x_{ip}}^2 + A_{4k}{x_{iq}}^2 + A_{5k}x_{ip}x_{iq} \tag{2}$$

where, $p, q = 1, 2, \ldots, m$, $p \neq q$, $k$=1,2,...,$\frac{1}{2}m(m-1)$ The coefficients $A_{0k}$, $A_{1k}$, ... in equation (2) are determined by solving the following minimization problem for each $p$, $q$ and $k$:

$$Min\left\{\sum_{i=1}^{n_{tr}} (y_{i+20} - z_k(x_{ip}, x_{iq}))^2\right\} \tag{3}$$

**Step 3 :** Evaluate each partial description $z_k$ in the following way. Firstly, the "accuracy" of each partial description is measured by the following criterion where the regularity criterion ($J_k$) is used to avoid over-fitting of the model to the measured data and to provide the minimum number of selection layers in multi-layered GMDH algorithm.

$$J_k = \sqrt{\frac{\sum_{i=n_{tr}+1}^{n} (y_{i+20} - z_{ik})^2}{\sum_{i=n_{tr}+1}^{n} (y_{i+20})^2}} \tag{4}$$

where, $z_{ik}$ denotes the output of the $k$-th partial description in the case that the $i$-th data is applied. Next, the threshold $R_l$ is defined for the $l$-th layer based on the parameter $T$ given as follows:

$$T = \sum_{i=1}^{n} (y_{i+20} - \bar{y}_{i+20})^2 \Big/ \sum_{i=1}^{n} (y_{i+20})^2 \tag{5}$$

where, $\bar{y}_{i+20}$ is a mean value of $y_{i+20}$ ($i$=1,2,...$n$). In our case, $R_l$ was set to be $R_1 = 4.5T$, $R_2 = 3.5T$ and $R_3 = 2.5T$.... Based on this setup, the output $z_k$ of the $k$-th partial description, which meets the following regularity condition, is selected.

$$z_k \; whichmeets \; J_k < R_l$$
$$k = 1, 2, \ldots, \frac{1}{2}m(m-1), l = 1, 2, \ldots \tag{6}$$

**Step 4 :** Assume that the number of outputs of selected partial description is $r$. These selected $r$ variables are redefined as the input variables $x_k(k = 1, 2, \ldots r)$ for the next layer.

**Step 5 :** Calculate the following parameter $\theta_l$, which decides the termination of the evolution of the layer. If $\theta_{l+1} > \theta_l$ holds, then terminate; otherwise, increment $l$ and go to Step 2.

$$\theta_l = \min_k J_k, k = 1, 2, \ldots r \tag{7}$$

The best partial description in the last layer is regarded as the estimated model $\hat{y}_{i+20} = \hat{f}(x_{i1}, x_{i2}, \ldots, x_{im})$.

The data of the third trial of the four drivers were used for the modeling. A part of the profile between the beginning of the deceleration and the final stopping point of each driver shown in Figs. 3(a) and (b) was used.

In our case, $m$=3 in the GMDH as described in Sect. 3, i.e. $x_{i1}$, $x_{i2}$, $x_{i3}$ and the braking output $y_{(i+20)2}$ is regarded as

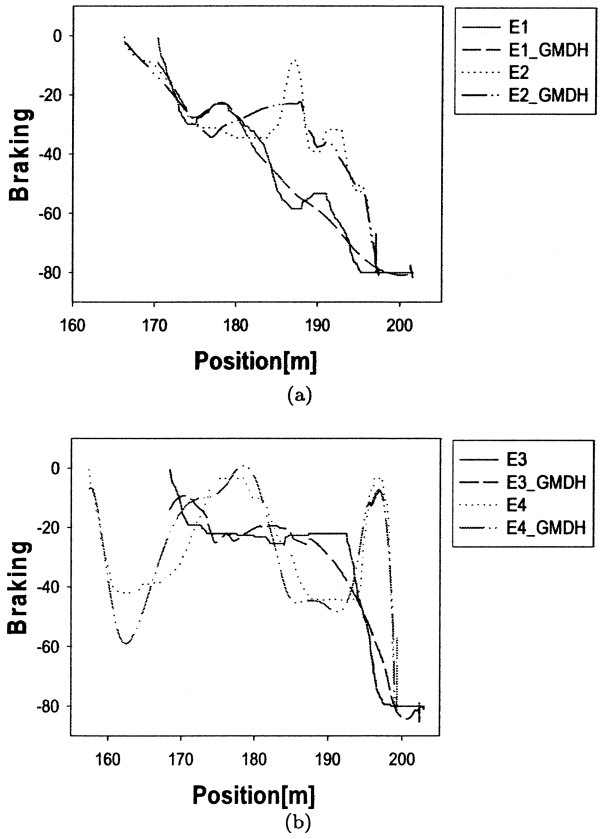


**Fig. 5** Comparison of actual brake output and estimated brake output under the 2D environment.

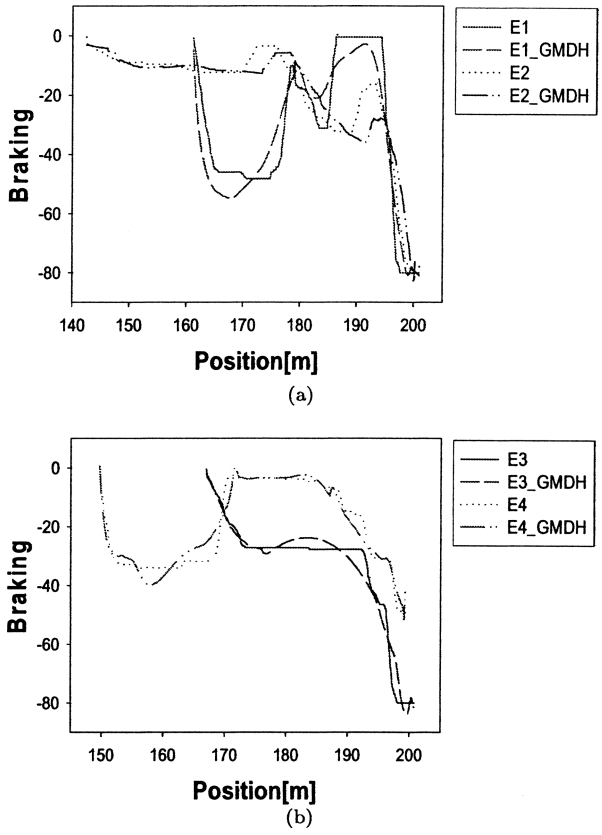


**Fig. 6** Comparison of actual brake output and estimated brake output under the 3D environment.

the single output. Before applying the GMDH to the measured data, the input and output data are normalized as follows:

$$\bar{x}_{ij} = \begin{cases} \frac{x_{ij}}{x_{ijmax}} & (x_{ij} \geq 0) \\ -\frac{x_{ij}}{x_{ijmin}} & (x_{ij} < 0) \end{cases} \tag{8}$$

$$x_{ij} \in [x_{ijmin}\ x_{ijmax}]$$

$$\bar{y}_{(i+20)j} = \begin{cases} \frac{y_{(i+20)j}}{y_{(i+20)jmax}} & (y_{(i+20)j} \geq 0) \\ -\frac{y_{(i+20)j}}{y_{(i+20)jmin}} & (y_{(i+20)j} < 0) \end{cases} \tag{9}$$

$$y_{(i+20)j} \in [y_{(i+20)jmin}\ y_{(i+20)jmax}]$$

Also, a low-pass filter is applied to the acceleration data to reduce the noise components. The transfer function of the first-order low-pass filter has the following form:

$$G(z) = \frac{S(z)}{1 + z^{-1}Sz} \tag{10}$$

$$S(z) = \frac{\tau^{-1}}{1 - z^{-1}}, \tau = f_s \Big/ 2\pi f_c$$

where, $f_s$ and $f_c$ are the sampling and cut-off frequencies and their values are 100 [Hz] and 15 [Hz], respectively.

According to the procedure, the GMDH has evolved until the second layer, and the final model of the braking maneuver was represented by the fourth-order polynomial, which is a function of three inputs as follows:

$$\begin{aligned} \hat{y}_{(i+20)2} &= a_1 + a_2 x_{i1} + a_3 {x_{i1}}^2 + a_4 {x_{i1}}^3 \\ &+ a_5 {x_{i1}}^4 + a_6 x_{i2} + a_7 {x_{i2}}^2 + a_8 {x_{i2}}^3 \\ &+ a_9 {x_{i2}}^4 + a_{10} x_{i3} + a_{11} {x_{i3}}^2 + a_{12} {x_{i3}}^3 \\ &+ a_{13} {x_{i3}}^4 + a_{14} x_{i1} x_{i2} + a_{15} {x_{i1}}^2 {x_{i2}}^2 \\ &+ a_{16} x_{i1} x_{i3} + a_{17} {x_{i1}}^2 {x_{i3}}^2 + a_{18} x_{i2} x_{i3} \\ &+ a_{19} {x_{i2}}^2 {x_{i3}}^2 + a_{20} x_{i1} {x_{i2}}^2 + a_{21} x_{i1} {x_{i2}}^3 \\ &+ a_{22} {x_{i1}}^2 x_{i2} + a_{23} {x_{i1}}^3 x_{i2} + a_{24} x_{i1} {x_{i3}}^2 \\ &+ a_{25} x_{i1} {x_{i3}}^3 + a_{26} {x_{i1}}^2 x_{i3} + a_{27} {x_{i1}}^3 x_{i3} \\ &+ a_{28} x_{i2} {x_{i3}}^2 + a_{29} {x_{i2}}^2 x_{i3} + a_{30} x_{i1} x_{i2} x_{i3} \\ &+ a_{31} {x_{i1}}^2 x_{i2} x_{i3} + a_{32} x_{i1} {x_{i2}}^2 x_{i3} \\ &+ a_{33} x_{i1} x_{i2} {x_{i3}}^2 \quad (i = 1, 2, \ldots, n) \end{aligned} \tag{11}$$

To verify the validity of the obtained model, the reproduced brake output, which is calculated using the model, and the measured brake output are plotted in Figs. 5 and 6. Note that the amount of braking takes negative values in Figs. 5 and 6, and zero braking implies "no braking."

As shown in Figs. 5 and 6, the measured brake output and reproduced brake output based on GMDH agree well. These results verify the effectiveness of the modeling based on GMDH.

Next, the coefficients in polynomials for examinees E1 and E3 under the 2D and 3D environments are listed in Tables 4 to 7, respectively. In Tables 4 to 7, the coefficients of variables are arranged in the order of magnitude.

In Tables 4 to 7, the most dominant input information

**Table 4** Variables and coefficient values for a polynomial expression of E1 examinee under the 2D environment.

| Variables | Coefficient values | Variables | Coefficient values |
|---|---|---|---|
| $x_{i1}^2$ | −98388.821 | $x_{i1}x_{i2}^3$ | −35.721 |
| $x_{i1}^3$ | 74978.043 | $x_{i2}x_{i3}$ | −34.699 |
| $x_{i1}$ | 57060.436 | $x_{i2}^3$ | 33.856 |
| $x_{i1}^4$ | −21312.278 | $x_{i1}x_{i3}^2$ | −29.621 |
| $a_1$ | −12338.398 | $x_{i1}^2x_{i3}^2$ | 17.433 |
| $x_{i1}^3x_{i2}$ | −2147.674 | $x_{i2}^2x_{i3}$ | 12.248 |
| $x_{i1}x_{i2}$ | −1942.774 | $x_{i3}^2$ | −12.104 |
| $x_{i1}^2x_{i3}$ | 1823.238 | $x_{i1}x_{i2}^2x_{i3}$ | 11.990 |
| $x_{i1}^2x_{i2}$ | 1747.387 | $x_{i2}^4$ | −5.975 |
| $x_{i1}x_{i3}$ | −1663.029 | $x_{i1}x_{i2}x_{i3}$ | 2.643 |
| $x_{i2}$ | 1556.777 | $x_{i1}x_{i2}x_{i3}^2$ | −1.093 |
| $x_{i1}x_{i2}^2$ | 1366.758 | $x_{i2}x_{i3}^2$ | −1.036 |
| $x_{i1}^2x_{i2}^2$ | −665.110 | $x_{i2}^2x_{i3}^2$ | −0.365 |
| $x_{i1}^3x_{i3}$ | −659.046 | $x_{i3}^3$ | −0.167 |
| $x_{i2}^2$ | −501.557 | $x_{i1}x_{i3}^3$ | 0.163 |
| $x_{i3}$ | 498.779 | $x_{i3}^4$ | −0.002 |
| $x_{i1}^2x_{i2}x_{i3}$ | −35.839 | | |

**Table 5** Variables and coefficient values for a polynomial expression of E3 examinee under the 2D environment.

| Variables | Coefficient values | Variables | Coefficient values |
|---|---|---|---|
| $x_{i1}^2$ | −204486.618 | $x_{i2}x_{i3}$ | −2084.794 |
| $x_{i1}$ | 154088.280 | $x_{i1}^2x_{i2}x_{i3}$ | −2084.576 |
| $x_{i1}^3$ | 119764.931 | $x_{i1}x_{i3}^2$ | 917.882 |
| $x_{i1}x_{i2}$ | −86950.537 | $x_{i3}^2$ | −488.704 |
| $x_{i1}^2x_{i2}$ | 79628.238 | $x_{i1}^2x_{i3}^2$ | −429.691 |
| $a_1$ | −43261.986 | $x_{i2}^3$ | 397.621 |
| $x_{i2}$ | 31497.647 | $x_{i1}x_{i2}^3$ | −384.157 |
| $x_{i1}^4$ | −26105.618 | $x_{i2}x_{i3}^2$ | 115.595 |
| $x_{i1}^3x_{i2}$ | −24175.319 | $x_{i1}x_{i2}x_{i3}^2$ | −111.681 |
| $x_{i1}x_{i3}$ | −15713.491 | $x_{i1}x_{i2}^2x_{i3}$ | −76.614 |
| $x_{i1}^2x_{i3}$ | 14571.539 | $x_{i2}^2x_{i3}$ | 74.028 |
| $x_{i1}x_{i2}^2$ | 12825.631 | $x_{i1}x_{i3}^3$ | −20.419 |
| $x_{i2}^2$ | −6717.372 | $x_{i3}^3$ | 19.729 |
| $x_{i1}^2x_{i2}^2$ | −6114.707 | $x_{i2}^4$ | −7.059 |
| $x_{i3}$ | 5605.146 | $x_{i2}^2x_{i3}^2$ | −4.104 |
| $x_{i1}^3x_{i3}$ | −4463.381 | $x_{i3}^4$ | −0.546 |
| $x_{i1}x_{i2}x_{i3}$ | 4171.837 | | |

**Table 6** Variables and coefficient values for a polynomial expression of E1 examinee under the 3D environment.

| Variables | Coefficient values | Variables | Coefficient values |
|---|---|---|---|
| $x_{i1}^2$ | −46585.055 | $x_{i2}x_{i3}$ | −78.789 |
| $x_{i1}^3$ | 32163.824 | $x_{i1}^2x_{i2}x_{i3}$ | −76.586 |
| $x_{i1}$ | 30055.795 | $x_{i1}x_{i3}^2$ | −11.581 |
| $x_{i1}^4$ | −8349.771 | $x_{i1}x_{i2}^3$ | −11.103 |
| $x_{i1}^2x_{i2}$ | 7902.786 | $x_{i2}^3$ | 10.925 |
| $x_{i1}x_{i2}$ | −7743.618 | $x_{i1}^2x_{i3}^2$ | 7.027 |
| $a_1$ | −7285.800 | $x_{i3}^2$ | 4.706 |
| $x_{i1}^3x_{i2}$ | −2689.039 | $x_{i1}x_{i2}x_{i3}^2$ | 2.352 |
| $x_{i2}$ | 2529.818 | $x_{i2}x_{i3}^2$ | −2.315 |
| $x_{i1}^2x_{i3}$ | 1613.742 | $x_{i2}^2x_{i3}$ | 1.732 |
| $x_{i1}x_{i3}$ | −1590.340 | $x_{i1}x_{i2}^2x_{i3}$ | −1.657 |
| $x_{i1}x_{i2}^2$ | 618.666 | $x_{i3}^3$ | −0.627 |
| $x_{i1}^3x_{i3}$ | −546.803 | $x_{i1}x_{i3}^3$ | 0.600 |
| $x_{i3}$ | 523.656 | $x_{i2}^4$ | −0.120 |
| $x_{i1}^2x_{i2}^2$ | −314.757 | $x_{i2}^2x_{i3}^2$ | 0.050 |
| $x_{i2}^2$ | −304.044 | $x_{i3}^4$ | −0.009 |
| $x_{i1}x_{i2}x_3$ | 155.431 | | |

**Table 7** Variables and coefficient values for a polynomial expression of E3 examinee under the 3D environment.

| Variables | Coefficient values | Variables | Coefficient values |
|---|---|---|---|
| $x_{i1}^2$ | −116336.283 | $x_{i2}^2$ | 607.249 |
| $x_{i1}^3$ | 83812.334 | $x_{i1}x_{i3}^2$ | 545.858 |
| $x_{i1}$ | 71219.529 | $x_{i1}^2x_{i2}^2$ | 444.806 |
| $x_{i1}^4$ | −22502.636 | $x_{i1}^2x_{i3}^2$ | −279.146 |
| $a_1$ | −16195.004 | $x_{i3}^2$ | −267.894 |
| $x_{i1}^2x_{i3}$ | 11353.739 | $x_{i2}^3$ | −82.823 |
| $x_{i1}x_{i3}$ | −11141.015 | $x_{i1}x_{i2}^3$ | 81.070 |
| $x_{i1}^2x_{i2}$ | 10090.726 | $x_{i1}x_{i2}^2x_{i3}$ | −45.962 |
| $x_{i1}x_{i2}$ | −7886.068 | $x_{i2}^2x_{i3}$ | 44.396 |
| $x_{i1}^3x_{i2}$ | −4099.566 | $x_{i2}x_{i3}^2$ | 34.025 |
| $x_{i1}^3x_{i3}$ | −3864.918 | $x_{i1}x_{i2}x_{i3}^2$ | −33.305 |
| $x_{i3}$ | 3651.357 | $x_{i1}x_{i3}^3$ | −9.738 |
| $x_{i2}$ | 1896.054 | $x_{i3}^3$ | 9.406 |
| $x_{i1}x_{i2}x_{i3}$ | 1547.754 | $x_{i2}^4$ | 2.392 |
| $x_{i1}x_{i2}^2$ | −1054.861 | $x_{i2}^2x_{i3}^2$ | −1.965 |
| $x_{i1}^2x_{i2}x_{i3}$ | −778.731 | $x_{i3}^4$ | −0.208 |
| $x_{i2}x_{i3}$ | −768.448 | | |

is the distance $x_1$ to the stop line, and the second dominant one is the velocity $x_2$. On the other hand, the acceleration $x_3$ has less importance in the stopping maneuver. From the obtained model, it has been found that the braking operation has higher dependency on the velocity information than the acceleration information.

However, we can also see that the dependency on the acceleration in the 3D case was higher than the 2D case. This result implicitly shows the effect of the stereoscopic vision. If we use the Driving Simulator with some motion, the dependency on the acceleration will be higher than these cases. A similar tendency is also found for the data of the other examinees. These results are expected to provide us with the information needed to analyze the behaviors of drivers. Note that some coefficients take large values in Tables 4 to 7.

However, the expressions of the complex polynomials are usually not unique, i.e. some factorized form can be another candidate to express the polynomials. In our case, since one physical variable (for example, $x_{i1}$) appear many times in many different terms, the factorized form may give more reasonable understanding. As the concluding remarks, the GMDH can be used to capture the meaning of driving behavior at least roughly associating with each variable although the rigorous understanding of each term in the GMDH model is somewhat unclear. More clear understanding of the model will be investigated in our future works.

## 6. Conclusions

This paper has presented the analysis of the stopping maneuver of the human driver by using a new three-dimensional driving simulator that uses CAVE, which provides stereo-

scopic immersive vision. First of all, the difference in the stopping maneuver between 3D and 2D virtual environments has been investigated, and the usefulness of providing the 3D virtual environment has been demonstrated. GMDH has been applied to the measured data in order to build a mathematical model of the driving behavior. Although the rigorous understanding of each term in the GMDH model is somewhat unclear, the GMDH can be used to capture the meaning of driving behavior at least roughly associating with each variable. From the obtained model, it has been found that acceleration information has less importance in the stopping maneuver, compared with distance and velocity information. In the future, the obtained model will be used to design the vehicle control systems that accommodate with the driver's behavior. Also, physiologicaland psychological factors will be integrated into our work in order to build more complex human models.

## Acknowledgement

This work was supported by the Space Robotic Center of the Toyota Technological Institute, where CAVE is installed. The authors would like to thank Dr. Yoji Umetani and the researchers involved at the Space Robotic Center for their helpful suggestions. The authors also would like to thank Dr. Yasushi Amano, of Toyota Central Research and Development Labs, for his valuable advices.

### References

[1] A. Kawashima, K. Kobayashi, K. Watanabe, and N. Numata, "Modeling on the mental stress and automobile driving," SICE, vol.38, no.1, pp.26–34, Jan. 2002.
[2] Y. Matsuura and T. Morioka, "An analysis of the difference threshold of driver's visual senses and bodily sensations on a simulator," SAEJ, vol.32, no.3, pp.95–99, July 2001.
[3] K. Satoh, T. Wakasugi, and K. Hiramatsu, "Accuracy and feeling of simulated cues on the JARI driving simulator," Toyota Central R&D Labs. Report, pp.35–43, 1998.
[4] S. Nagiri, Y. Amano, K. Fukui, S. Doi, and M. Akamatsu, "The analysis of the driver behavior for the development of driver support system," Toyota Central R&D Labs. Report, pp.1–14, 2001.
[5] A. Kemeny and F. Panerai, "Evaluation perception in driving simulation experiments," TRENDS in cognitive Sciences, vol.7, no.1, pp.31–37, 2003.
[6] M.T. Schultheis and R.R. Mourant, "Virtual reality and driving: The road to better assessment for cognitively impaired populations," Presence by MIT, vol.10, no.4, Aug. 2001.
[7] M. Akamatsu, S. Doi, M. Okuwa, and K. Takuguchi, "Behavior based human environment creation technology," Project International Workshop on ITS Human Interface, Japan (ITS HMI symposium 2000).
[8] S. Doi, S. Nagiri, and Y. Amano, "Research and development of driving support system for individual driving ability," Toyota Central R&D Labs. Report, pp.71–107, 1998.
[9] H. Summala, D. Lamble, and M. Laakso, "Driving experience and perception of the lead car's braking when looking at in -car targets," Accid. Anal. and Prev., vol.30, no.4, pp.401–407, 1998.
[10] I. Siegler, G. Reymond, A. Kemeny, and A. Berthoz, "Sensorimotor integration in a driving simulator: Contributions of motion cueing in elementary driving tasks," Proc. Driving Simulation Conference DSC'2001, pp.1–12, Nice, Sept. 2001.
[11] F. Panerai, J. Droulez, J-M. Kelada, A. Kemeny, E. Balligand, and B. Favre, "Speed and safety distance control in truck driving: Comparison of simulation and real-world environment," Proc. Driving Simulation Conference DSC'2001, pp.91–107, Paris, France, 2001.
[12] H. Uno and K. Hiramatsu, "Aged driver's avoidance capabilities in an emergent traffic situation," SAEJ, vol.32, no.1, pp.113–118, Jan. 2001.
[13] K. Yamada and T. Wakasugi, "A study on effectiveness of forward vehicle collision warning," SAEJ, vol.32, no.1, pp.119–124, Jan. 2001.
[14] E.R. Boer, T. Yamamura, N. Kuge, and A. Girshick, "Experiencing the same road twice: A driver centered comparison between simulation and reality," DSC2000 (Driving Simulation Conference), pp.15–28, Paris, France, 2000.
[15] J. Pierce, Expanding the Interaction Lexicon for 3D Graphics, Carnegie Mellon University, Feb. 2000.
[16] A.L. Alexander and C.D. Wickens, "The effects of spatial awareness biases on maneuver choice in a cockpit display of traffic information," 12th International Symposium on Aviation Psychology, pp.1–6, Dayton, OH, 2003.
[17] H.B.-L. Duh, "An 'independent visual background' reduced balance disturbance evoked by visual scene motion: Implication for alleviating simulator sickness," SIGCHI'01, pp.85–89, Seattle, USA, April 2001.
[18] S.V.G. Cobb, S. Nichols, A. Ramsey, and J.R. Wilson, "Virtual reality-induced symptoms and effects (VRISE)," Presence, vol.8, no.2, pp.169–186, April 1999.
[19] S.J. Farlow, Self-Organizing Method in Modeling, Marcel Decker USA, 1984.
[20] I. Hayashi and H. Tanaka, "The fuzzy GMDH algorithm by possibility models and its application," Fuzzy Sets Syst., vol.36, pp.245–258, 1990.
[21] S. Inaba, Traffic Accident and Human Engineering, Books Corona JAPAN, 1988.
[22] D.M. Hawkins, "The problem of overfitting," J. Chem. Inf. Comput., vol.44, no.1, pp.1–12, 2004.
[23] T.I. Akasyonova, V.V. Volkovich, and I.V. Tetko, "Robust polynomial neural networks in quantative-structure activity relationship studies," Systems Analysis Modeling Simulation, vol.43, no.10, pp.1331–1339, Oct. 2003.
[24] D.W. Kim, B.W. Kim, and G.T. Park, "A plasma-etching process modeling via a polynomial neural network," ETRI J., vol.26, no.4, pp.297–306, Aug. 2004.

**Jong-Hae Kim** was born in Ulsan, Korea, in 1968. He received the M.E. and Ph.D. degrees in Electrical Engineering from Yeungnam University, Korea in 1996 and 1999, respectively. He is currently working toward the Ph.D. degree at the Department of Electrical Engineering, Nagoya University, Japan. His researh interests are in the area of resonant inverter, soft switching technology, virtual reality and hybrid dynamical systems.

**Yoshimichi Matsui** was born in Aichi, Japan, in 1978. He received the B.E. and M.E. degrees in Electrical Engineering from Nagoya University, JAPAN in 2001 and 2003, respectively. He is currently working toward the Ph.D. degree at the Department of Electronics and Information Engineering, Nagoya University, Japan. His researh interests include virtual reality and hybrid dynamical systems.

**Soichiro Hayakawa** was born in Aichi, Japan, in 1968. He received the Ph.D. degree in Electrical Engineering from Nagoya University, Japan in 1996. Since 1996, he has been an Assistant Professor at Toyota Technological Institute, Japan. His researh interests are in the area of motion control systems, robotics, virtual reality and hybrid dynamical systems. Dr. Hayakawa is a member of the IEEJ and SICE.

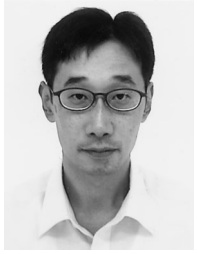

**Tatsuya Suzuki** He was born in Aichi, Japan, in 1964. He received the B.E., M.E. and Ph.D. degrees in Electronic Mechanical Engineering from Nagoya University, Japan in 1986, 1988 and 1991, respectively. From 1998 to 1999, he was a visiting researcher of the Mechanical Engineering Department of U.C.Berkeley. He is currently an Associate Professor of the Department of Electronic-Mechanical Engineering of Nagoya University. He won the paper award from IEEJ in 1995. His researh interests are in the area of motion control systems, hybrid dynamical systems, scheduling and so on. Dr. Suzuki is a member of the IEEJ, SICE, RSJ, JSME and IEEE.

**Shigeru Okuma** was born in Gifu, Japan, in 1948. He received the B.E., M.E. and Ph.D. degrees in Electronic-Mechnical Engineering from Nagoya University, Japan in 1970, 1972 and 1978, respectively. He also received the M.E. degree in systems engineering from Case Western Reserve University, Cleveland, OH, in 1974. Since 1990, he has been a Professor in Department of Electrical Engineering and Computer Science, Nagoya University. His researh interests are power elctronics, robotics and evolutionary soft computing. Dr. Okuma was the recipient of the IEEE IECON'92 Best Paper Award, in addition to paper awards from the Japan Society for Precision Engineering and Institute of Electrical Engineering of Japan.

**Nuio Tsuchida** was born in Aichi, Japan, in 1943. He received the Ph.D. degree in the Department of Electrical and Electronics Engineering of Nagoya University, Japan in 1972. From 1972 to 1982, he was an Assistant Professor in the Department of Electrical and Electronics Engineering, Nagoya University. Since 1992, he has been a Professor at Toyota Technological Institute. His researh interests are micro actuator, sensor and robotics. Dr. Tsuchida is a member of the IEEJ and IEJ.